Discover Materials

Discover

Brief Communication

Dissolution behaviour and imageability of ternary borate glasses for use in geniculate artery embolization

R. A. Manchester[1] · T. Z. Todorova[2] · E. Tonkopi[3] · B. Kelly[4] · J. Gosse[4] · C. Davis[4] · K. Brewer[1,4] · M. Shymka[5] · D. Boyd[1,2,3]

Received: 18 May 2021 / Accepted: 5 August 2021
Published online: 16 September 2021

Abstract
Sixteen borate glass compositions comprising K_2O and SrO were screened, using a design of mixtures approach, to model compositional effects on dissolution, CT imageability, and MRI relaxivity (R_2). Based on the characteristics of each network, together with dose determination and toxicological risk, the composition identified as BKSA16 was selected as a preferred composition for pre-clinical evaluations related to geniculate artery embolization (GAE). Accordingly, BKSA16 particles were subjected to a flame spheroidization process and recharacterized, including the evaluation of residual mass at 72 h in physiologically representative media along with clinical determinations of suspension time (ease of use). For both the irregular particles and microspheres residual mass was present at 72 h in physiologically representative media. Additionally, both the microspheres and irregular particles achieved suspension times deemed to be acceptable for clinical use. The collective data confirms that BKSA16 microspheres have a range of beneficial features (specifically both degradable and imageable) suited to GAE.

Keywords Borate glass · Radiopacity · Mixture Designs · Dissolution · Geniculate Artery Embolization

1 Introduction

Osteoarthritis (OA) is a common, chronic, and debilitating condition affecting the synovial joint [1]. Substantial limitations with existing treatments have driven intensive research intended to identify new therapies using a 'treat-to-target' approach [2–4]. One emerging treat-to-target option is known as geniculate artery embolization (GAE) [5–7]. GAE was developed for patients who are resistant to conservative therapies and not yet indicated for a knee replacement [6]. GAE is a transcatheter based clinical intervention *(ca. 80 min)* that targets abnormal angiogenesis [6] which facilitates the growth of new unmyelinated sensory nerves inducing pain signalling and sensitization [4, 8]. Based on this mechanistic understanding, and the treat-to-target nature of GAE, it has been clinically demonstrated to provide substantial pain relief for patients [5, 7].

GAE requires embolic microspheres to generate vessel occlusion. However, at this point in time, there exists no microspheres designed to meet the demands of this clinical intervention. The ideal embolic microspheres for GAE should possess several features including, in the first instance, the ability to degrade in situ. It has been determined that degradable microspheres (i) ameliorate clinical risks by ensuring no long-term presence in the body, (ii) facilitate vessel recanalization

✉ D. Boyd, d.boyd@dal.ca | [1]School of Biomedical Engineering, Dalhousie University, Halifax, NS, Canada. [2]Department of Applied Oral Science, Faculty of Dentistry, Dalhousie University, Halifax, NS, Canada. [3]Department of Diagnostic Radiology, Dalhousie University, Halifax, NS, Canada. [4]BIOTIC, IWK Health Centre, Halifax, NS, Canada. [5]School of Medical Sciences, Dalhousie University, Halifax, NS, Canada.

post treatment(s), and (iii) allow flexibility for repeat embolization procedures if necessary [9–11]. Furthermore, patients have an overwhelming preference for technologies which are eliminated from the body on completion of such treatments. Coupled with degradation, it is considered beneficial to have microspheres that exhibit certain imageability characteristics. For example, it may be beneficial to have microspheres with intrinsic x-ray attenuation characteristics *(for intraprocedural imaging),* while also exhibiting appropriate MRI relaxation characteristics *(so as not to confound follow-up imaging on MRI)* [12]. The expanded selection criteria for an ideal GAE microsphere can be described as (i) ensuring no residual mass remains in situ after *ca.* 72 h, with (ii) a particle size distribution (PSD) of 100–300 µm, (iii) a density of < 2.4 g/cm^3, and (iv) preferably a suspension time of ≥ 2 min. These design inputs were gathered through one-on-one interviews with users and leading experts in the field via two mechanisms; firstly, through independent third-party interviews conducted by TL Health (PA, USA) and via direct interaction of the researchers with users at relevant international conferences (including the European Conference on Interventional Oncology, Global Embolization Symposium and Technologies, and Cardiovascular and Interventional Radiological Society of Europe).

The purpose of this work is to characterize the dissolution behaviour and imageability of 16 borate glasses, and to identify a preferred composition which best addresses the ideal design features of an embolic microsphere for GAE. Additional data relating to the systematic evaluation of the physical and chemical characteristics of this glass system are available elsewhere in the literature [13].

2 Materials and Methods

Sixteen glass compositions *(including five replicates for statistical purposes)* were established (Table 1) using Design-Expert Software (Version 12.0.9) based on an *I-optimal* approach [13]. Each composition was synthesized using a melt quench technique and subjected to baseline characterization (density, x-ray diffraction (XRD), ^{11}B MAS NMR, and differential scanning calorimetry (DSC)) as described elsewhere [13]. Glasses were synthesized with analytical grade boric anhydride (99.98% trace metals basis and CAS number 1303–86-2), strontium carbonate (≥ 99.9% trace metals basis and CAS number 1633–05-2), and potassium carbonate (≥ 99% trace metals basis and CAS number 584–08-7) (Sigma-Aldrich, USA). Each composition was melted in a 100 mL Pt crucible (XRF Scientific, Montreal) and were subsequently placed at room temperature and subjected to a ramp rate of 25 ℃/min to 600 ℃ for 60 min. Thereafter, the ramp rate was increased to 20 ℃/min until 1200 ℃ was achieved as the final dwell temperature and held for 60 min [13]. Samples were then stored under desiccated conditions prior to experimentation.

Dissolution experiments for each glass were conducted in two stages. Firstly, glasses were subjected to screening, using sterile saline as the dissolution media, to identify chemistries with desirable mass loss characteristics. Individual

Table 1 BKSA compositions (with five replicate compositions 1 and 13, 4 and 8, 5 and 7, 6 and 12, and 9 and 10) by mol% as characterized in Manchester et al. [13]

Glass Identified	B_2O_3	K_2O	SrO
BKSA 1*	69.00	30.00	1.00
BKSA 2	75.79	8.74	15.47
BKSA 3	90.00	8.28	1.73
BKSA 4•	83.55	15.45	1.00
BKSA 5$^+$	69.00	15.53	15.47
BKSA 6†	69.00	1.00	30.00
BKSA 7$^+$	69.00	15.53	15.47
BKSA 8•	83.55	15.45	1.00
BKSA 9■	79.37	1.00	19.63
BKSA 10■	79.37	1.00	19.63
BKSA 11	69.00	8.24	22.76
BKSA 12†	69.00	1.00	30.00
BKSA 13*	69.00	30.00	1.00
BKSA 14	82.72	8.93	8.35
BKSA 15	90.00	1.00	9.00
BKSA 16	73.91	20.40	5.69

Symbols represent replicates

Corning® 15 ml centrifuge tubes were weighed in triplicate with 10 mL saline (0.9% Sodium chloride, Baxter, Illinois, USA). 0.1 g of each glass composition (100–300 µm) was placed in falcon tubes (n = 3 per composition for each media) and then in a shaking incubator (120 RPM and 37 °C for 2 h) then immediately centrifuged (3.0 RCF/ 4.4 RPM) for 15 min. The supernatant was decanted from the pellet and the pellet (in the original test tube) was dried (50 °C for 96 h) then weighed to determine the average residual mass. The preferred glass (BKSA16) was subjected to residual mass experiments in physiologically representative media using a mass: volume ratio of 0.1 g (glass) to 10 mL of 10% bovine calf serum (BCS)/90% Dulbecco's Modified Eagle Medium (DMEM) (Sigma Aldrich, USA). Residual mass was determined after 72 h using the same conditions as described for the screening stage.

Each composition was imaged on a clinical CT scanner Somatom Definition AS + (Siemens Healthineers, Erlangen, Germany) at 70 and 120 kVp using 400 mAs, pitch = 0.5, and 1 mm slice thickness [12]. Both full and half strength Omnipaque 350 (Iohexol; 350 mg of non-ionic iodine per mL, GE Healthcare Ireland, Cork, Ireland) were used as controls. Radiopacity measurements was reported as Hounsfield Units (HU) ± standard deviation (SD) [12].

MRI susceptibility was established for each composition by dispersing the materials (100–300 µm) in a non-aqueous gel made with 1% Evonik Intelimer IPA 13–1 NG polymer in peanut oil (2, 4, 6, 8, 10% w/w, n = 5). The gels were then loaded in 5 mm tubes and exposed to magnetic stirring, horizontal rotation, and heating before cooling on ice to solidify the gel. Each composition was measured at room temperature using Agilent 3 T preclinical MRI to obtain R_2 (CPMG) MRI relaxometry measurements. A linear regression analysis and extrapolation to 100% volume fraction was used to provide values for the particles [12].

Irregular BKSA16 particles (100–300 µm), were subjected to flame spheroidization using a propane oxygen flame to transform the morphology of the glass frit to a microsphere (described elsewhere [14]). After processing the glass microspheres were packaged dry clean containers and sterilized using gamma irradiation (average dose 30 kGy, Nordion, Ontario, Canada).

Scanning Electron Microscopy (SEM) was conducted on BKSA16 microspheres (BKSA16M). A Hitachi S4700 Cold Field Emission scanning electron microscope (with an Oxford Analytical 80 mm SDD detector for energy dispersive x-ray spectroscopy) was used to image the microspheres with a condenser lens 1 set to 3, an emission current of 20 mA, and accelerating voltage of 10 kV. Prior to imaging the specimens, they were placed on aluminum stubs and coated with gold–palladium (20 nm) to prevent product contamination [9].

Following spheroidization of BKSA16 from irregular particles (BKSA16I) to microspheres (BKSA16M), the samples were recharacterized (density, XRD, ^{11}B MAS NMR, and DSC) as previously described in Manchester et al. [13]**.** The data pre- [13] and post-spheroidization was compared to determine the impact of spheroidization on the material.

The suspension time of BKSA16 microspheres was qualitatively determined using accepted methods from the relevant clinical literature [15]. Succinctly, 0.1 g of glass (100–300 µm) placed into sealed 15 mL tubes with 10 mL of Omnipaque 350 (n = 3). Once added, a timer was started, and the tubes were inverted (10x) to create a suspension. Subsequently, the falcon tubes were held upright, placed against a black background and monitored until the suspension fell below 2/3 of the total volume [15]. The time was then averaged for three runs to determine the average suspension time.

3 Results

Average residual mass at 2 h (n = 3) was assessed in saline is presented in Fig. 1A. From these data a cubic model with statistical significance (p-value < 0.0001) was established (Table 2). The average residual mass at 2 h ranged from 7 to 108% (where a value > 100% represents a residual mass greater than the initial mass used). The ranking of factors that facilitate an increase in the final residual mass are B > K*Sr > Sr > K > B*Sr > B*K, where B*K and B*Sr result in a decrease in the final residual mass.

CT radiopacity (n = 5) at 70 kVp (Fig. 1B) produced a statistically significant (p-value < 0.0001) reduced quadratic model (Table 2). CT Radiopacity (70 kVp) ranged from 212 to 5249 HU. Analysis of the coefficients at 70 kVp (Table 2) resulted in the following ranking of factors that lead to an increase in radiopacity: Sr > K > B > B*Sr > K*Sr. CT radiopacity (n = 5) at 120 kVp (Fig. 1C) produced a statistically significant (p-value < 0.0001) reduced cubic model (Table 2). CT Radiopacity (120 kVp) ranged from 161 to 3600 HU. Analysis of the coefficients at 120 kVp (Fig. 1C) ranked the factors driving an increase in radiopacity as: Sr > K*Sr > K > B > B*Sr > B*K. Notably, interactions B*K and B*Sr resulted in a reduction in CT radiopacity.

Analysis of the R_2 slope (n = 2) for MRI (Fig. 1D) provided a statistically significant (p-value 0.0152) reduced cubic model (Table 2) with values ranging from 1.298 to 21.12. Analysis of the coefficients for the R2 slope (Table 2)

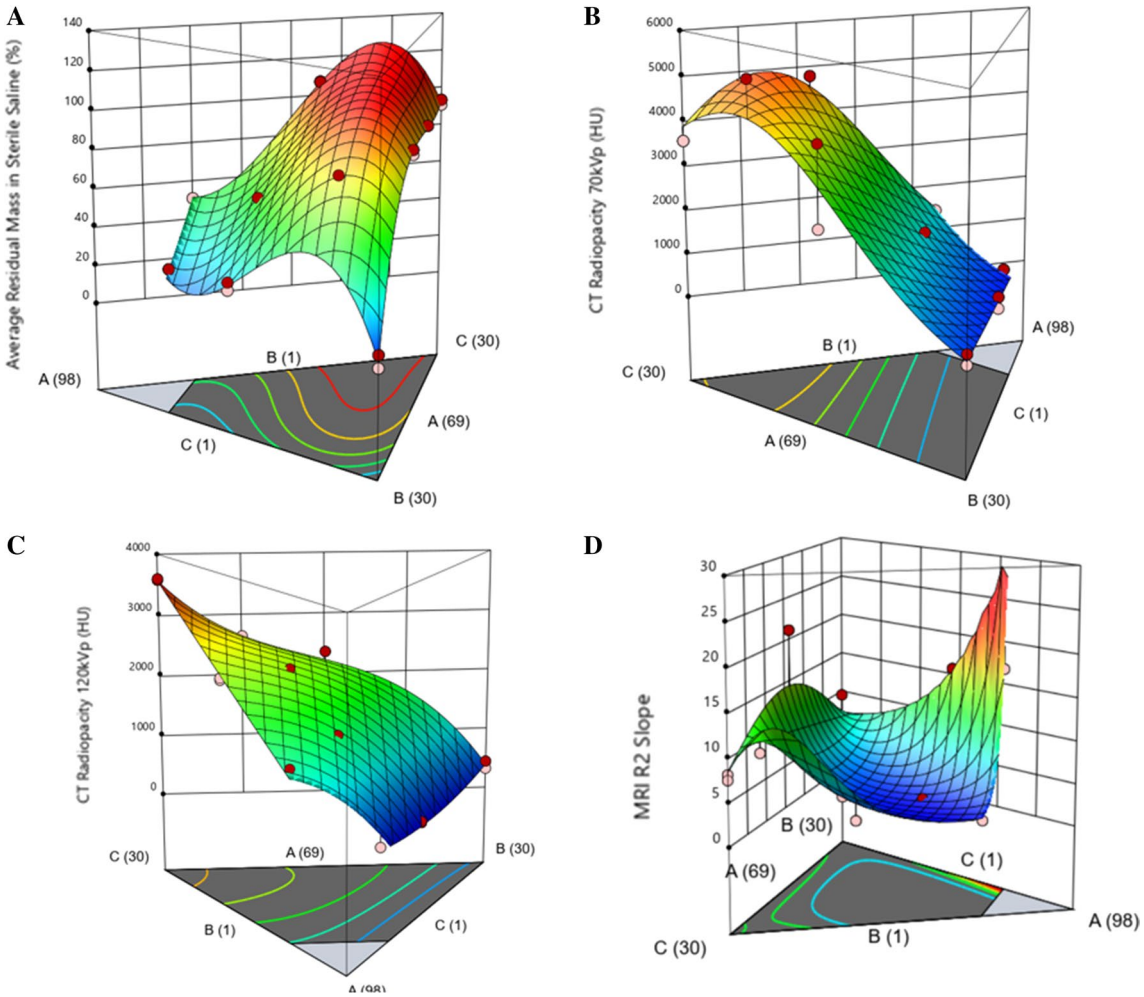

Fig. 1 Contour plots of responses for **A** average residual mass at 2 h in sterile saline, **B** radiopacity at 70 kVp. **C** CT radiopacity at 120 kVp, and **D** MRI R2 slope. The x-axes are labelled as 'A': mol% B_2O_3, 'B': mol% K_2O, and 'C': mol% SrO

resulted in the ranking of factors for increased slope (i.e., higher relaxivity) as follows: B > K*Sr > Sr > K > B*K > B*Sr (where B*K and B*Sr decrease slope).

BKSA16 was processed into microspheres and morphology was confirmed via SEM imaging (Fig. 2A). Imaging confirmed the absence of irregular particles, surface contamination or other adverse findings. For completeness, and to account for any changes in the chemical and physical properties arising from microspheres processing, the irregular particles (BKSA16I) and microspheres (BKSA16M) had their basic characteristics (methods described elsewhere [13]) compared (Table 2).

BKSA16I and BKSA16M were compared based on residual mass in saline after 2 h (Fig. 2B). BKSA16I achieved a residual mass of 84.25 ± 5.04% and BKSA16M achieved a residual mass of 88.44 ± 4.1% after 2 h. Average residual mass (n = 3) for the irregular particles (BKSA16I) and microspheres (BKSA16M) were also evaluated in 10% BCS/90% DMEM at 72 h (Fig. 2C). Notably, BKSA16 had residual mass at 72 h in both forms (irregular particles and microspheres). Finally, the average suspension time (n = 3) for BKSA16I was determined to be 2.01 min (run 1: 2.05 min, run 2: 1.20 min, and run 3: 1.58 min). The average suspension time for BKSA16M was determined to be 1.15 min (run 1: 1.11 min, run 2: 1.18 min, and run 3: 1.17 min).

Table 2 Model equations and model statistics for each response per Fig. 1 and data for density, XRD (% crystallinity), ^{11}B MAS NMR (B[3]: B[4]), and DSC (T_g onset and inflection) pre- [13] and post-spheroidization of BKSA16

Response	Regression Models	R^2	$R^2_{adjusted}$	$R^2_{predicted}$	Prob > F	C.V. (%)
Model statistics						
Average Residual Mass (2 h screen)	$+143.19B_2O_3+10.37K_2O+92.92SrO-196.32B_2O_3{*}K_2O-161.39B_2O_3{*}SrO+139.83K_2O{*}SrO$	0.9978	0.9944	0.9479	299.46	4.02
CT 70 kVp	$+5.58B_2O_3+6.24K_2O+8.22SrO+4.82B_2O_3{*}SrO+3.31K_2O{*}SrO$	0.9464	0.9269	0.8920	48.53	3.80
CT 120 kVp	$+389.14B_2O_3+401.69K_2O+3568.03SrO-1047.05B_2O_3{*}K_2O-71.46B_2O_3{*}SrO+1005.86K_2O{*}SrO$	0.9940	0.9889	0.9676	165.01	7.73
MRI R2 Slope	$+4.56B_2O_3+1.88K_2O+2.01SrO-2.49B_2O_3{*}K_2O-10.62B_2O_3{*}SrO+2.41K_2O{*}SrO$	0.8247	0.6713	0.2596	5.38	26.56

BKSA16	Density	% Crystallinity	B[3]: B[4]	T_g Onset (°C)	T_g Inflection (°C)
BKSA16 Pre- and Post-Spheroidization					
Irregular Particle (BKSA16I)	2.322	0.2	61:39	464.5	475.1
Microsphere (BKSA16M)	2.301	5.9	68:32	428.5	437.2

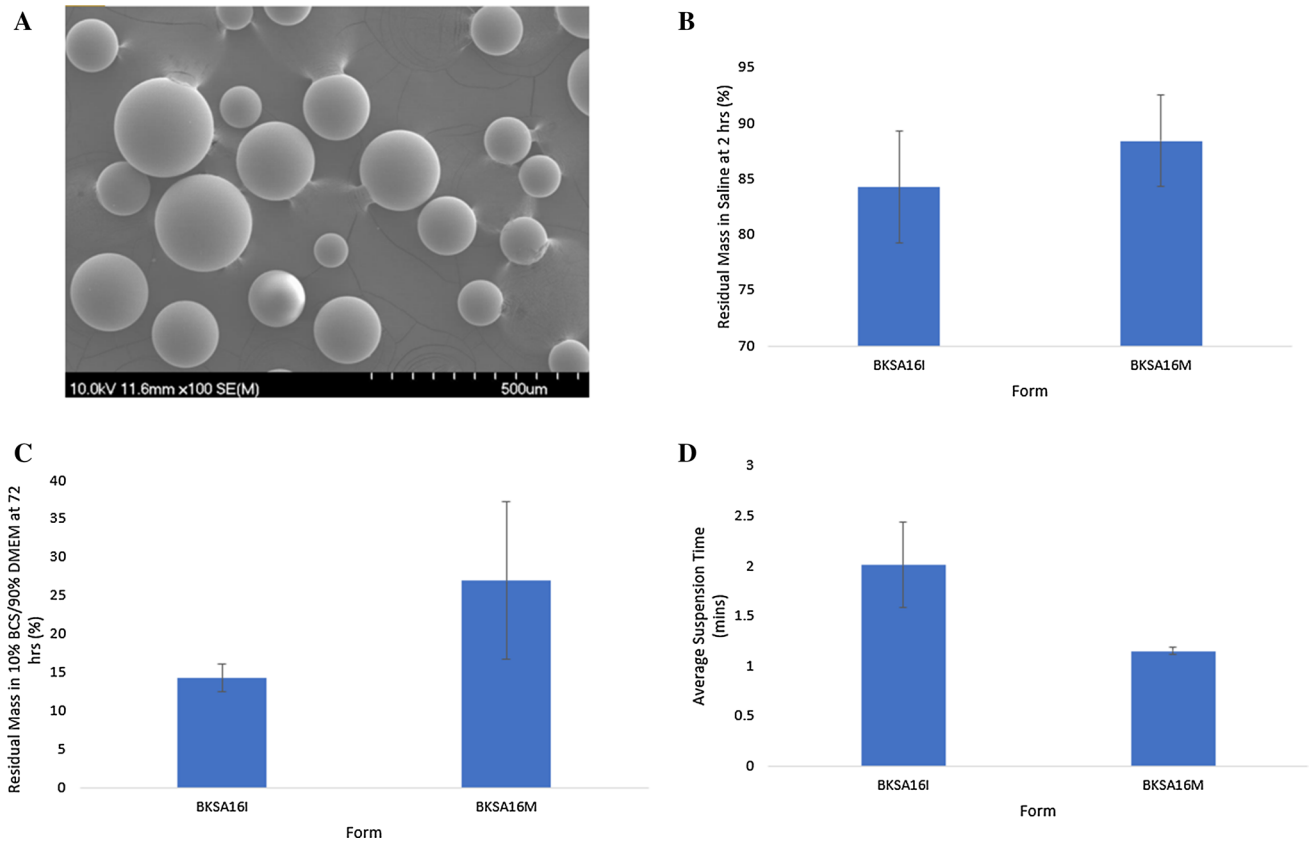

Fig. 2 **A** SEM image of BKSA16 microspheres (100x), **B** residual mass in saline at 2 h for BKSA16I and BKSA16M, **C** residual mass in 10% BSC/90% DMEM at 72 h for BKSA16I and BKSA16M, and **D** suspension times for BKSA16I and BKSA16M

4 Discussion

Average residual mass in saline (Fig. 1A) lead to the elimination of seven compositions (BKSA1, 3, 4, 8, 13, 14, and 15) as they achieved *ca.* < 50% residual mass at 2 h. This decision was informed from previous work where mass loss in vitro was a significant underestimate of in vivo dissolution rates [9, 12]. As such these compositions have a low probability of clinical success based on dissolution requirements. It was determined that radiopacity sufficient for clinical use can be achieved in glasses with high mol% SrO (Fig. 1B and C) such as, BKSA6, 7, 9, 10, 11, and 12. These compositions achieve radiopacity comparable to microspheres deemed sufficient for clinical imaging in the literature. For example, Negussie et al., and Ashrafi et al., have established imageable particles as having attenuation values of > 3972 HU and 4718 HU respectively [16, 17]. Additionally, Contour™ particles in half strength contrast have reported attenuation values of *ca.* 2500 HU [18]. Similarly, BKSA6, 7, 9, 10, 11, and 12 exhibit CT radiopacity values in the range 3563–5249 HU at 70 kVp. SrO was found to be the largest driver of increased CT radiopacity and responsible for facilitating a larger residual mass following dissolution experiment (Table 2). As such control of this critical constituent is an important consideration in materials design. Imageability on MRI was also assessed (Fig. 1D) and the compositions were shown to induce minimal R_2 contrast changes and as such, these particles will not confound follow-up R_2-weighted MRI scans in a clinical setting as required [12].

Considering the data from our previous work [13] and in conjunction with dissolution and imageability findings, BKSA16 was selected as it best addressed the GAE microsphere requirements, and was further evaluated. While it has low CT radiopacity, BKSA16 also has a relatively low concentration of SrO *(5.69 mol%)* and B_2O_3 *(73.91 mol%)* which facilitates potential increases in the clinical unit dose (from 44 to 55.91 mg (Shymka 2021)) without raising toxicological concerns *(BKSA16 margin of safety (where > 1 indicates low toxicological risk) at 44 mg dose: boron = 1.27 and strontium = 1.67* (Shymka 2021)*)*. Due to the novelty of the procedure, there currently exists no cleared/approved products with a defined dose and as a result the dosing for this indication remains ambiguous. Nevertheless, on the basis of the existing clinical data which confirm doses within the range of *ca.* 0.2 mL [6, 7], it can be estimated that a probable dose for GAE will be in

the range of 44–55 mg (Shymka 2021). For the purposes of this work, a 44 mg dose was established based on the unit dose administered (0.2 ml Embozene particles) in clinical studies [7], a particle size of 100 µm, and a density of 2.3 g/cm^3 (Shymka 2021). Additionally, BKSA16 has a density of *ca.* 2.3 g/cm^3 *(comparable to a range of commercially available contrast media)* which will support adequate suspension, reduced sedimentation/aggregation, and ease of delivery [19]. Finally, BKSA16 has sufficient mass remaining (84.25% at 2 h) which should be adequate to support residual mass > 2 h in vivo and thereby, reduce the risk of ineffective occlusion [20]. To overcome the potential issues of low intrinsic CT radiopacity, these particles may be delivered via traditional TAE methods using half strength contrast to safely and effectively image the particles in a clinical setting and as such address this design requirement [21].

Following the selection of BKSA16, the irregular particles were processed into microspheres (Fig. 2A) and characterized (Table 2). The properties pre/post spheroidization were absent of major differences. As such, the properties of BKSA16 are stable, and these particles can be made into microspheres substantial without alteration of the glass properties. The residual mass in saline at 2 h was also compared between the BKSA16 irregular particles (BKSA16I) and microspheres (BKSA16M) (Fig. 2B). No major differences in dissolution occurred when comparing the two forms and both forms maintained a residual mass at 2 h which will facilitate effective occlusion of the vasculature. The dissolution of BKSA16I and BKSA16M was further assessed in 10% BCS/90% DMEM to provide insight into their dissolution behaviour in vivo and both forms were found to have a residual mass of 14.28 and 26.99% at 72 h, respectively (Fig. 2C). The dissolution of borate networks has become an area of interest in the literature, and while our understanding is nascent in this regard, it has been suggested that hydrolysis and hydration drive dissolution of such networks in aqueous media [22]. However, benchtop models have been shown to significantly overestimate mass loss rates in comparison to animal models *(e.g. 100% dissolution ca. 48 h and ca. 24 h, respectively)* [9, 12]. Thus, it may be appropriate to suggest 100% dissolution will likely occur *in* vivo in < 72 h meeting the requirements for a microsphere indicated for GAE, however, further animal studies are required to fully characterize the dissolution behaviour of BKSA16 in situ. Lastly, the suspension times of BKSA16I and BKSA16M were assessed and compared to microspheres currently used in TAE procedures (*ca.* 2 min) [17, 23]. BKSA16I achieved a consistent suspension time with commercially available microspheres used in TAE's procedures and BKSA16M settled out of solution quicker (*ca.* 1.20 min). However, as stated in Johnson et al. [24] a shorter suspension time of *ca.* 30 s is still considered sufficient for clinical use, can support the delivery of the particles (with similar handling when compared to drug loaded DC Bead), and is disregarded as a "clinical concern when sufficient soluble contrast media is used" [24]. As such, BKSA16 is able to sustain a suspension time that is compatible for use clinically. While the data are preliminary and further studies are required, BKSA16 remains a promising candidate for use as an embolic microsphere indicated for GAE.

5 Conclusions

Glasses based on B_2O_3, K_2O and SrO were systematically evaluated as potential degradable embolic materials for GAE using a statistical design methodology. Modulation of critical properties across a range of clinical variables were assessed (e.g., dissolution, CT-radiopacity, MRI R_2 relaxivity, and suspension times). Based on the data, one exemplary composition (BKSA16) was processed into spherical form, and no substantive changes to critical properties were observed as a result of processing. BKSA16 is a promising candidate for use as a degradable embolic microsphere indicated for GAE and warrants further development and investigation.

Acknowledgements The authors would like to acknowledge the financial support of both the Natural Sciences and Engineering Research Council (NSERC) Discovery and Innovacorp (Early Stage Commercialization Fund) ESCF programs. The authors also thank Mr. John Cusmina (TL Health, USA) for interviewing clinical specialists to provide inputs on the design parameters discussed in this paper. In addition, the authors are thankful to Dr Bob. Abraham, Dr. Mark Filiaggi, and Dr. Brendan Leung for their invaluable inputs to this project, and to Dr Ulrike Werner Zwanziger for providing NMR support to this paper.

Authors' contributions Conceptualization: [RM, DB], Methodology: [RM, TT, DB], Formal analysis: [RM, TT, ET, KB, DB], Investigation: [RM, TT, ET, JG, CD, BK, KB, DB], Writing-Original Draft: [RM, MS], Writing-Review & Editing: [RM, TT, ET, KB, MS, DB], Visualization [RM], Project administration: [RM, DB], Validation: [TT], Resources: [DB], Supervision: [DB], Funding acquisition: [DB]. All authors read and approved the final manuscript.

Data availability The authors declare that all datasets [tables and figures] in this current study are available from the corresponding author on reasonable request.

Declarations

Competing interests The authors declare no competing interests.

References

1. Hunter DJ, Bierma-Zeinstra S. Osteoarthritis. Lancet. 393(10182): 1745–1759. doi: https://doi.org/10.1016/S0140-6736(19)30417-9.
2. Kolasinski SL, et al. 2019 American College of Rheumatology/Arthritis Foundation Guideline for the Management of Osteoarthritis of the Hand, Hip, and Knee. Arthritis Care Res. 2020;72(2):149–62. https://doi.org/10.1002/acr.24131.
3. Migliore A, et al. It is the time to think about a treat-to-target strategy for knee osteoarthritis. Ther Clin Risk Manag. 2019;15:1479–82. https://doi.org/10.2147/TCRM.S221562.
4. Malfait A-M, Schnitzer TJ. Towards a mechanism-based approach to pain management in osteoarthritis. Nat Rev Rheumatol. 2013;9(11):654–64. https://doi.org/10.1038/nrrheum.2013.138.
5. Bagla S, Piechowiak R, Hartman T, Orlando J, Del Gaizo D, Isaacson A. Genicular artery embolization for the treatment of knee pain secondary to osteoarthritis. J Vasc Interv Radiol. 2019. https://doi.org/10.1016/j.jvir.2019.09.018.
6. Okuno Y, Korchi AM, Shinjo T, Kato S. Transcatheter arterial embolization as a treatment for medial knee pain in patients with mild to moderate osteoarthritis. Cardiovasc Intervent Radiol. 2015;38(2):336–43. https://doi.org/10.1007/s00270-014-0944-8.
7. Okuno Y, Korchi AM, Shinjo T, Kato S, Kaneko T. Midterm clinical outcomes and mr imaging changes after transcatheter arterial embolization as a treatment for mild to moderate radiographic knee osteoarthritis resistant to conservative treatment. J Vasc Interv Radiol. 2017;28(7):995–1002. https://doi.org/10.1016/j.jvir.2017.02.033.
8. Ashraf S, Wibberley H, Mapp PI, Hill R, Wilson D, Walsh DA. Increased vascular penetration and nerve growth in the meniscus: a potential source of pain in osteoarthritis. Ann Rheum Dis. 2011;70(3):523–9. https://doi.org/10.1136/ard.2010.137844.
9. Doucet J, MacDonald K, Lee C, Hana RA, Soulez G, Boyd D. The feasibility of degradable glass microspheres as transient embolic medical devices. J Biomater Appl. 2021;35(6):615–32. https://doi.org/10.1177/0885328220944871.
10. Doucet J, et al. Advances in degradable embolic microspheres: a state of the art review. J Funct Biomater. 2018;9(1):14. https://doi.org/10.3390/jfb9010014.
11. Owen RJ, Nation PN, Polakowski R, Biliske JA, Tiege PB, Griffith IJ. A preclinical study of the safety and efficacy of Occlusin™ 500 artificial embolization device in sheep. Cardiovasc Intervent Radiol. 2012;35(3):636–44. https://doi.org/10.1007/s00270-011-0218-7.
12. Doucet J, et al. Multi-modal imageability and degradation characteristics of high-borate glass systems for transient embolization. J Non-Cryst Solids. 2019;510:26–35. https://doi.org/10.1016/j.jnoncrysol.2019.01.014.
13. Manchester RA, Todorova TZ, Werner-Zwanziger U, Boyd D. Mixture designs to investigate the role of alkali and alkaline earth cations on composition-structure-property relationships in ternary borate glass networks. J Non-Cryst Solids. 2021;569: 120982. https://doi.org/10.1016/j.jnoncrysol.2021.120982.
14. Kehoe S, et al. Effects of γ-irradiation and accelerated aging on composition-structure–property relationships for radiopaque embolic microspheres. J Non-crystalline Solids. 2014;402:84–90. https://doi.org/10.1016/j.jnoncrysol.2014.05.016.
15. Lewis AL, et al. Comparative in vitro evaluation of microspherical embolisation agents. J Mater Sci Mater Med. 2016;17(12):1193–204. https://doi.org/10.1007/s10856-006-0592-x.
16. Negussie AH, et al. Synthesis, characterization, and imaging of radiopaque bismuth beads for image-guided transarterial embolization. Sci Rep. 2021;11(1):533. https://doi.org/10.1038/s41598-020-79900-z.
17. Ashrafi K, et al. Characterization of a novel intrinsically radiopaque Drug-eluting Bead for image-guided therapy: DC Bead LUMI™. J Controlled Release. 2017;250:36–47. https://doi.org/10.1016/j.jconrel.2017.02.001.
18. Kehoe S, Tonkopi E, Abraham RJ, Boyd D. "Predicting the thermal responses and radiopacity of multicomponent zinc–silicate bioglasses: A focus on ZnO, La2O3, SiO2 and TiO2. J Non-crystalline Solids. 2012;358:3388–95. https://doi.org/10.1016/j.jnoncrysol.2012.08.024.
19. Caine M, Carugo D, Zhang X, Hill M, Dreher MR, Lewis AL. Review of the development of methods for characterization of microspheres for use in embolotherapy: translating bench to cathlab. Adv Healthc Mater. 2017;6(9):1601291. https://doi.org/10.1002/adhm.201601291.
20. Maeda N, et al. Targeting and recanalization after embolization with calibrated resorbable microspheres versus hand-cut gelatin sponge particles in a porcine kidney model. J Vasc Interv Radiol. 2013;24(9):1391–8. https://doi.org/10.1016/j.jvir.2013.05.058.
21. Sharma KV, et al. Development of 'Imageable' Beads for Transcatheter Embolotherapy. J Vasc Interv Radiol. 2010;21(6):865–76. https://doi.org/10.1016/j.jvir.2010.02.031.
22. George JL, Brow RK. In-situ characterization of borate glass dissolution kinetics by μ-Raman spectroscopy. J Non-Cryst Solids. 2015;426:116–24. https://doi.org/10.1016/j.jnoncrysol.2015.07.003.
23. Hu J, et al. Advances in biomaterials and technologies for vascular embolization. Adv Mater. 2019;31(33):1901071. https://doi.org/10.1002/adma.201901071.
24. Johnson CG, et al. Preparation of radiopaque drug-eluting beads for transcatheter chemoembolization. J Vasc Interv Radiol. 2016;27(1):117-126.e3. https://doi.org/10.1016/j.jvir.2015.09.011.